

Supporting Information for

Uterine Epithelial Organoids Reveal Insights into Epithelial Specification and Plasticity in Development and Disease

Jason A. Rizo, Vakil Ahmad, Jacob M. Pru, Sarayut Winuthayanon, Sridevi Challa, Tae Hoon Kim, Jae-Wook Jeong, Thomas E. Spencer*, and Andrew M. Kelleher*

*Corresponding Authors: Andrew M. Kelleher, andrew.kelleher@missouri.edu; Thomas E. Spencer, spencerte@missouri.edu

This PDF file includes:

SI Methods

Figures S1 to S5

Tables S1 to S4

Datasets S1 to S4 (description)

SI References

SI METHODS

Mouse female reproductive tract organoids

Oviducts, uterine horns, and cervixes were dissected from C57BL/6J mice. Uterine horns were cut into 3 pieces and digested in 1% trypsin (Sigma, T4799) in calcium and magnesium-free HBSS (Gibco, 14175-095) for 45 minutes at 4°C followed by 45 minutes at 37°C using an orbital shaker. The digestion was stopped with 1% soybean trypsin inhibitor (Gibco, 17075-029) in HBSS with 5 mM MgCl₂ and 0.1 mg/mL DNase-I (Roche, 10104159001). For PNDs 3, 5, 7 (n= 4-6 mice/biological replicate; n= 5-18 biological replicates per PND), Pasteur pipettes were carefully forged to create a slightly smaller diameter than the uterus, and endometrial epithelial sheets were retrieved by gentle suction using a mouth pipette. For PNDs 12 and 15 (n= 2-3 mice/biological replicate; n= 5-18 biological replicates per PND), the digested uterine horns were gently squeezed with #5 forceps. PND3 oviducts and cervixes (n= 5-8 mice/biological replicate; n= 3 biological replicates per organ type) were digested overnight using Liberase (0.2 mg/mL; Roche, 5401119001) diluted in phenol red-free RPMI 1640 medium supplemented with DNase-I (0.5 mg/mL; Roche, 10104159001) using an orbital shaker. The cell pellets from each organ were rinsed gently with Base Organoid Media (Table S1) and plated in 25 cm² flasks (Greiner Bio-One, 690195). Unattached epithelia were removed from flasks following 30 minutes of culture. After centrifugation (300 x g for 3 minutes) and washing, epithelium pellets were resuspended in 80% Cultrex (R&D Systems, 3445-005-01) and 20% organoid expansion media (Table S2). Organoids were passaged (1:3 ratio) every 7-10 days. For passaging, Cultrex/organoid drops were detached from the cell culture plate and organoids were dissociated by gentle pipetting and transferred into 1.5 mL Eppendorf tubes. After centrifugation (300 x g for 3 minutes), the supernatant was removed, replaced by 1.5 µL of base organoid media, and pipetted up and down to dissociate the pellet. Following an additional centrifugation step, the organoid pellet was resuspended in Cultrex (1:3 ratio; 180 µL per well of organoids) and plated in 12-well plates (15 µL drops; 4 drops per well). Cultrex drops were incubated at 37 °C for 15 min prior to adding 800 µL of organoid expansion media per well. Organoid cryopreservation was performed with freezing

medium consisting of 10% DMSO in fetal bovine serum (FBS, Sigma, F0926) as described previously(1). Brightfield images were captured on a Leica DMI8 inverted microscope and Leica K8 camera using Leica Application Suite X (LAS X). EEO number (n= 5-8 drops/biological replicate) and frequency of structures $[(\# \text{ of ML EEO}) \div (\text{total } \# \text{ of EEO})]$ were analyzed using ImageJ (n= 3-5 biological replicates/PND) and the data are presented as the mean \pm SEM. Statistical differences between two groups were determined with Student's t-test (GraphPad Prism 9) and statistical significance was defined as $p < 0.05$.

Isolation and culture of uterine and cervicovaginal mesenchyme and skin fibroblast

Mesenchymal/fibroblast cells were isolated from the uterus, cervix/vagina, and skin of PND3 females. For uterine mesenchyme, the epithelium was first removed from the uteri of 4-6 mice as described above. Next, uteri, cervix/vagina, and skin were respectively pooled in 5 mL Eppendorf tubes, finely minced with small scissors, and digested overnight with Liberase (0.2 mg/mL; Roche, 5401119001) diluted in phenol red-free RPMI 1640 medium supplemented with DNase-I (0.5 mg/mL; Roche, 10104159001). Cervicovaginal and skin tissues were filtered through 20 μ m EASYstrainers (Greiner Bio-One, 07001105) to remove epithelial cells.

Mesenchymal/fibroblast cell pellets were then transferred to 25 cm² flasks (Greiner Bio-One, 690195) and cultured in stroma cell media (Table S3) at 37°C in a humidified 5% CO₂ environment. For cervicovaginal and skin mesenchyme/fibroblasts, the media was changed after 30 min to remove dead cells and contaminate epithelium. After reaching 80% confluency (usually within 72 h), cells were utilized for 2D or 3D co-culture experiments.

Endometrial epithelial organoid-mesenchyme 2D coculture

All 2D co-culture experiments were performed following the experimental design reported by Rizo et al. (1, 2) with some modifications. For 2D seeding, mesenchyme/fibroblast cells from PND3 female uterine, cervicovaginal, and skin tissues were detached with TrypLE (5 min, 37°C), washed with HBSS, and centrifuged (300 x g

for 3 min). Cervicovaginal and skin (but not uterine) cells were filtered through 20 μ M EASYstrainers, resuspended in 1.5 mL stromal cell medium, and plated into 6-well plates (200K cells/well). After 24 h, cells were gently rinsed with warm HBSS and a total of 3 mL of base organoid media were added to each well. For organoid establishment, endometrial epithelial cells were isolated from PND3 and PND15 mice (n= 5-18 biological replicates) the day after mesenchyme/fibroblast seeding into 6 well plates, as described above. Briefly, after the second round of centrifugation, cell pellets were resuspended in 90 μ L of 80% Cultrex: 20 % expansion media mix and divided into three 6-transwell inserts (0.4 μ m pores, Corning, 353090), each containing 2 drops of 15 μ L Cultrex mix. Inserts/Cultrex drops were then incubated at 37°C for 15 min. Next, the transwell inserts/Cultrex drops were placed into 6-well plates that either contained uterine/cervicovaginal mesenchyme, skin fibroblast or did not contain any cells. A total of 1.5 mL of mouse expansion media was added per insert. Fresh base organoid media (bottom, well) and expansion organoid media (top, insert) were added to each well and insert every 72 h. New primary mesenchyme/fibroblast cells were isolated and seeded every 5 days, and EEOs were passage into a new insert every 5-8 days. Co-cultures were documented every 5 days by brightfield microscopy, and EEO were collected for IF analysis following 20 days in culture. Images were taken with a Leica DMI8 inverted microscope and Leica K8 camera using Leica Application Suite X (LAS X).

Assembloid generation

To generate assembloids, uterine/cervicovaginal mesenchyme and skin fibroblast from PND3 females and endometrial epithelial cells from PND3 and PND15 mice were isolated with Liberase (0.2 mg/mL; Roche, 5401119001) diluted in phenol red-free RPMI 1640 medium supplemented with DNase-I (0.5 mg/mL; Roche, 10104159001). To ensure mesenchyme/fibroblast cell purity, cells were subjected to two rounds of magnetic separation using CD236 (EpCAM) microbeads following manufacturer's instructions (Miltenyi Biotec, 130105958). EpCAM⁺ epithelial cells bound to the magnetic columns were discarded and the flow-through containing the unlabeled mesenchyme/fibroblast was centrifuged (300 x g for 3 min) and resuspended in 1 mL of base organoid media. For assembly, a total of 3000 epithelial cells and 25000

mesenchymal/fibroblast cells were combined in each well with 250 μ L of base organoid media using 96-well low attachment plates (Fisher, 174929). For mesenchyme/fibroblast only controls, 20000 cells were seeded per well. For epithelial only controls, 10000 cells per well were seeded in 10% Cultrex (90% base organoid media). Cells were cultured at 37°C using a nutator (50 RPM) to facilitate the aggregation of cells. After 48 h, individual assembloids and stromal aggregates were transferred to 24-well low attachment plates (Corning, 3473) using wide-bore P1000 pipette tips and then cultured for another 6 days. Base organoid media (450 μ L) was changed every two days, and assembloid formation was monitored by brightfield microscopy. Assembloids and controls were collected following 8 days of culture for whole-mount staining. Each biological replicate contained n=6-10 assembloids; n=5 stromal aggregates; n=50-80 epithelial-only controls. All experiment were repeated in three independent biological replicates per mesenchymal/fibroblast cell type per PND. Image processing was performed using IMARIS v10.1.1. The proportion of single-layered (SL) and multilayered (ML) structures in epithelium-only controls was calculated based on p63 and KRT5 staining $[(\# \text{ of p63+}/\text{KRT5+ EEO}) \div (\# \text{ of CDH1+ EEO})]$. Statistical differences between two groups were determined with Student's t-test (GraphPad Prism 9) and statistical significance was defined as $p < 0.05$.

Human endometrial tissue and epithelial organoid culture

Endometrial epithelial organoids were isolated, cultured, and maintained as previously described (3, 4). For control samples, primary human endometrial epithelial cells were isolated from endometrial biopsies of premenopausal women with no history of endometrial pathology or endocrine disorders. All donors for control samples were not taking any steroid-modulating medications. Written informed consent was obtained from each donor and the study was approved by the University of Missouri Institutional Review Board (IRB Project Approval Number: 2011513). Cells were washed, resuspended in Cultrex BME, and plated in 15 μ L drops in 12-well plates. The Cultrex drops were then solidified by incubation at 37°C for 15 min before adding 800 μ L of human expansion media per well, as described (4). Organoid passaging and cryopreservation were performed as detailed in the mouse FRT organoid culture

section. Uterine endometrial cancer organoids were obtained from The University of Chicago Organoid Core after pathological grading of biopsies and cultured using standard practices. Uterine endometrial cancer tissue array (Cat. No. UT241, Tissuearray.com) was used for histological analysis and immunofluorescent staining.

Organoid and tissue preparation for histology

At least four organoid/Cultrex drops were examined per biological replicate. EEOs were incubated in a shaker (30 RPM) with 1 mL of Cell Recovery Solution (Corning, 354253) for 1 h at 4°C. EEO were then fixed using 4% EM grade paraformaldehyde (PFA; Electron Microscopy Sciences, 15710) for 15 min at room temperature (RT), stained with hematoxylin for 10 min, and washed 3-5 times with HBSS supplemented with 10% FBS to remove excess staining. EEOs were resuspended in 60 µL of 2% low-melting agarose (Fisher, BP16525) diluted in HBSS and quickly aliquoted (3-4 drops) on parafilm sheets (3 cm x 3 cm). After 3 minutes, the agarose droplets containing the EEO were sprayed with 70% ethanol to maintain humidity and incubated for 20 min at RT to let the agarose solidify. EEO drops were carefully transferred to tissue cassettes using forceps. For tissue processing, female reproductive tracts from 3-6 females were collected per PND and genotype. Tissues were fixed in 4% paraformaldehyde in PBS at 4°C overnight. EEO droplets and fixed tissues were dehydrated in ethanol, embedded in paraffin wax, and sectioned (7 µm) as previously described(2).

Immunofluorescence staining

Sections were mounted on slides, baked for 30 min at 60°C, deparaffinized in xylene, and rehydrated in a graded alcohol series (2). Deparaffinized sections were subjected to antigen retrieval by incubating sections in 1x Tris-EDTA buffer (Fisher, NC1627890) at 95°C for 15 min, followed by cooling to room temperature for 30 min. All slides were blocked with 2% (v/v) normal goat serum (NGS; Invitrogen, 01-6201) in PBS at room temperature for 1 h and incubated with primary antibodies (*SI Appendix*, Table S4) overnight at 4°C in blocking buffer. Immunofluorescence visualization was performed with Alexa 488 or Alexa 647-conjugated secondary antibodies (1:500 dilution; Jackson ImmunoResearch, #112-545-143, #111-605-144). Sections were counterstained with

Hoechst 33342 (2 µg/mL; Invitrogen, H3570) before affixing coverslips with ProLong™ Diamond Antifade Mountant (Invitrogen, 36961). Images were taken with a Leica DM6 B upright microscope and Leica K8 camera using Leica Application Suite X (LAS X).

Whole-mount staining

Assembloids/EEO were fixed using 4% PFA overnight at 4°C (EEO were fixed for 1 h) and washed three times with 0.1% PBS-Triton (PBST). Antigen retrieval was performed by incubation with FLASH2 reagent(5) at RT overnight with gentle shaking (20 RPM), followed by blocking buffer (10% FBS, 0.02% sodium azide, 1% BSA and 5% DMSO in PBST) for 2 h at RT, and then primary antibodies (*SI Appendix*, Table S4) diluted in blocking buffer for 48 h at 4°C. After washing with PBST 4-5 times, assembloids were incubated with Alexa 488 and 647 conjugated secondary antibodies (1:300 dilution) and Hoechst (1:1000) for 24 h at 4°C. Assembloids were washed with PBST 4-5 times, 20 min each, before mounting with clearing agent (60% glycerol and 2.5 M fructose). Confocal images were taken with a Leica TCS SP8 MP multiphoton microscope with diode lasers using Leica Application Suite X (LAS X).

Mass spectrometry analysis.

Mass spectrometry analysis was conducted by the Charles W. Gehrke Proteomics Center at the University of Missouri-Columbia. Uterine mesenchyme and skin fibroblast from PND3 females were isolated and cultured as described above (n= 6-8 mice per biological replicate). To analyze the secreted proteome, a total of 200K mesenchyme/fibroblast cells were seeded in 6 well plates and cultured in stromal cell media. After 24 h, cells were washed twice with warm HBSS to remove dead cells and 2 mL of fresh base organoid media were added per well. After 72 h, supernatants were collected, pooled (n= 3 wells per technical replicate), and centrifuged at 20000 × g for 10 min at 4°C. Samples were mixed with four volumes of 5% trichloroacetic acid in acetone and incubated at -20°C overnight (n= 3 technical replicates per biological replicate). Following centrifugation (20000 × g for 10 min at 4°C), samples were washed twice with 80% acetone and pellets were resuspended in 6 M urea, 2 M thiourea, and 100 mM ammonium bicarbonate, pH8.0 (n= 3 biological replicates per cell type). Protein

was quantified using the Pierce 660 nm Protein Assay method (Pierce Chemical, Dallas, TX, USA). Thirty micrograms of protein from each sample were reduced by 10 mM dithiothreitol and alkylated by 40 mM iodoacetamide, digested with LysC (mass spectrometry grade, Promega) at an enzyme to protein ratio of 1:70 and incubated for 3 h at 37°C. Trypsin (Promega) was added to the samples at a trypsin to protein (w/w) ratio of 1:50 and the samples were digested overnight at 37°C. Digested peptides were purified using Pierce C18 tips. To generate a spectra library, 1 µg purified peptides from each sample were combined, lyophilized, and resuspended in 5% acetonitrile, 0.1% formic acid. Samples were acquired on the Bruker timsTOF-Pro2 with the DIA-PASEF acquisition method using the 60 min liquid chromatography gradient. Proteins were identified and quantified using Spectronaut V18. The directDIA utility in Spectronaut, employing their Pulsar algorithm, was used to search the Uniprot-Mus database (17,963 entries, last update 2022). Data were filtered to remove all proteins identified in the blank sample (base organoid media) and saved as a tab-delimited text file. Data were imported into Perseus V1.16.15.0. Quantitation type of MS2 area was chosen and data filtering was set to Q value sparse. The DIA data were filtered with precursor FDR and protein group at 1%. A protein was considered present if identified in two samples per group and a MS2 quantity ≥ 10 in at least one sample. Benjamini-Hochberg-corrected T-tests were used to compare groups. Data were then exported to excel and log2 fold-change was calculated. Note for the purposes of fold-change calculation only (i.e., after T-tests) any 0 values were imputed with a value of 0.01 (Dataset S2, and Dataset S3). A *p*-value of ≤ 0.05 was considered significant.

Single cell isolation and RNA-sequencing and analysis

EEOs established from PND3 and PND15 females were collected after 8 days of culture (n=10 females/PND). EEOs were harvested, enzymatically dissociated using 0.05% trypsin (40 min, 37°C), and centrifuged at $300 \times g$ for 5 min. Cells were resuspended in Advanced DMEM/F12 medium supplemented with 1X antibiotic-antimycotic (Gibco, 15240062), passed through a 40 µm filter (Fisher, 087711) and pelleted ($300 \times g$ for 5 min). The cell pellets were then resuspended in 1 mL 0.04% BSA in PBS and counted to assess viability. Single-cell RNA sequencing was conducted at the University of

Missouri Genomics Technology Core as described previously (6). Briefly, single-cell droplet formation with a target count of 10,000 cells per sample was performed using the 10X Chromium system (10X Genomics; Pleasanton, CA). Sequencing was performed in paired-end mode using NovaSeq 6000 (Illumina).

Bioinformatic analysis of scRNA-seq data

For EEO scRNA-seq data analysis, the base call files were demultiplexed, processed to generate FASTQ files with Cell Ranger v7.2.0 (10X Genomics) command *mkfastq*, and then aligned to the mouse reference genome (GRCm39.110), followed by filtering and barcode and unique molecular identifier (UMI) counting to generate count matrices for each sample. The ALRA package (7) was used to impute cells following the standard pipeline. Seurat v5.1.0 (8) was used to do quality control and filtering using standard preprocessing workflow. Cells with unique feature counts under 200 (minimum 3 cells) and with greater than 10% mitochondrial counts were excluded. Previously published scRNA-seq datasets were downloaded from the NCBI database (accession codes GSE229790 (9) and PRJNA1046685 (6)) and processed using Seurat v5.1.0 (8) standard workflow. Data were integrated using Harmony (10) and Loupe Browser files were created using loupeR from 10X Genomics. Downstream transcription factors binding site analysis was determined with ChEA3 (11) using a database of publicly available ChIP-seq experiments and coexpression databases (Integrated meanRank) derived from literature. Gene ontology (GO) enrichment analysis of cluster markers and differentially expressed genes was performed using ShinyGO 0.80 (12). Hallmark gene sets for epithelial and mesenchymal cells were investigated using GSEA (13, 14). Raw FASTQ files from the GSE229790 (15) dataset were processed using the CeleScope pipeline (Singleron Biotechnologies), aligned to the mouse reference genome GRCm38.99, followed by filtering and barcode and unique molecular identifier (UMI) counting to generate count matrices for each sample. Standard single cell analysis workflow was performed as described above.

Mesenchymal-epithelial crosstalk analysis

CellChat (16) v.2.1.2 was used to infer cell-cell communication between neonatal uterine mesenchyme and epithelium using standard pipeline as previously described (17). Briefly, to identify potential interactions, the expression matrix was pre-processed using the in-built functions *identifyOverExpressedGenes*, *identifyOverExpressedInteractions*, and *projectData* with default parameters. Next, *computeCommunProb*, *computeCommunProbPathway*, and *aggregateNet* were used to infer the communication network and calculate communication probabilities. In addition, *filterCommunication* was used to remove cell-cell communication if there were fewer than 10 cells.

Endometrial cancer genomic data

Gene expression data associated with human endometrial cancer from The Cancer Genome Atlas (TCGA) consortium (18) were obtained from the R2 Genomic platform (<http://r2.amc.nl>; dataset: Uterine Corpus Endometrial Carcinoma-2022-v32) for 585 unique samples, from which 549 were Uterine Corpus Endometrial Carcinoma (UCEC) primary tumors and 35 were normal tissues. The R2 Limma statistical test was used to generate a list of DEGs between the two groups (fold-change > 2.5, FDR < 0.01). This list was compared to basal and luminal scRNA-seq expression data from PND3 EEOs. Human endometrioid endometrial cancer (EEC) scRNA-seq data were downloaded from NCBI database (PRJNA786266) (19). Data were subset and re-clustered by repeating the same workflow and mapped to the human genome GRCh38.110. Stroma and epithelial cells were identified based on expression of *PDGFRA*, *LUM*, *DCN*, and *COL6A3*, and *EPCAM*, *KRT8*, *KRT18*, and *KLF5* expression, respectively (*SI Appendix*, Dataset S4). Cells were then visualized primarily using UMAP nonlinear dimensional reduction from which feature and violin plots were generated to demonstrate the distribution and gene expression of selected genes.

Quantification and statistical analysis

All mouse and cell culture experiments were performed using at least three biological and technical replicates. The data are presented as the mean \pm SEM, as determined from at least three independent experiments. Following the Shapiro-WILK test for

normality, the data were analyzed using Student's t-test or ANOVA with Bonferroni correction (GraphPad Prism 9). A p-value of less than 0.05 was considered statistically significant. Statistical analyses for the genomic and proteomic experiments were performed using standard statistical tests as described above.

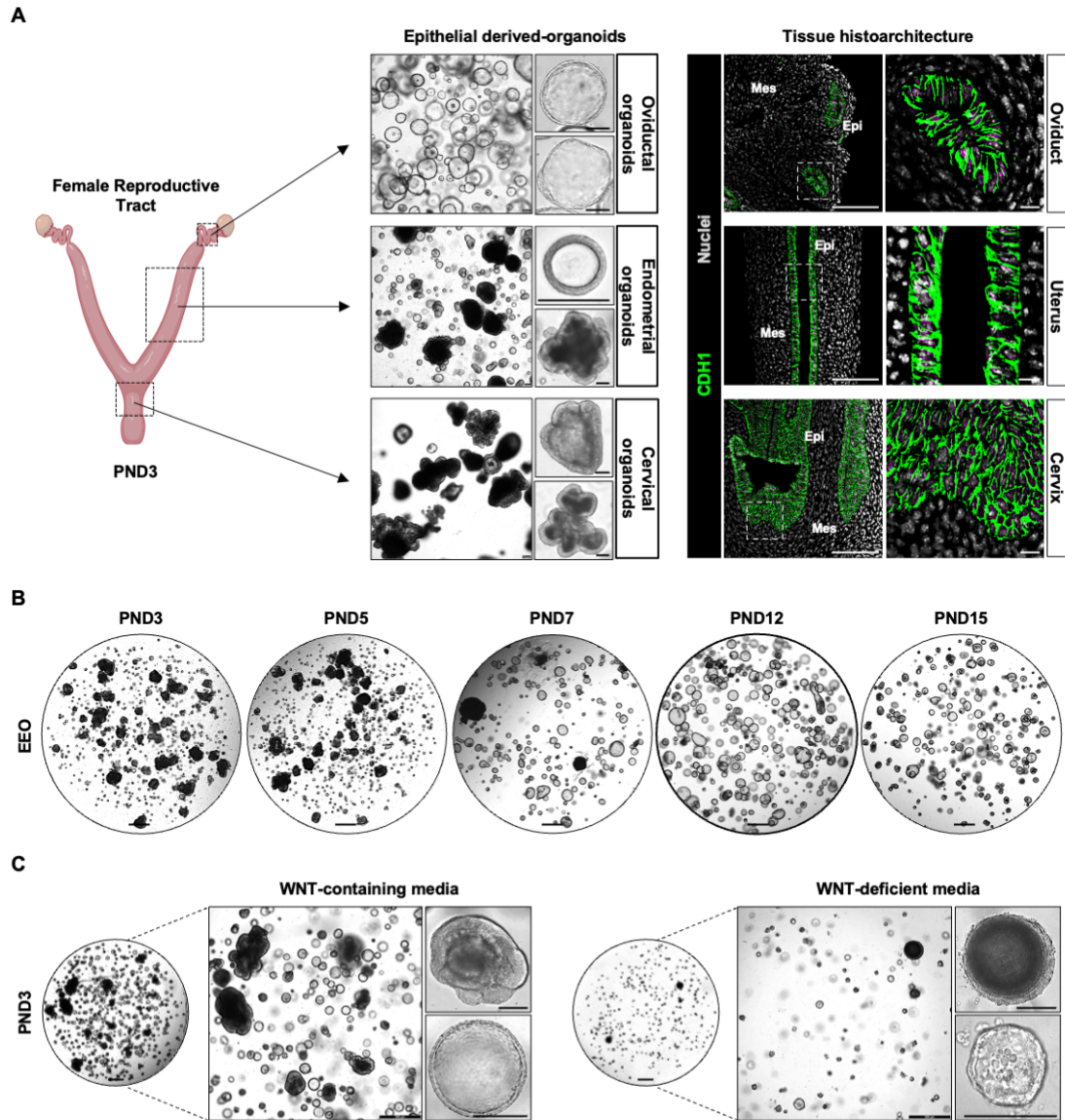


Figure S1. Establishment and characterization of neonatal uterine organoids.

(A) Illustration of female reproductive tract organoids established from postnatal day (PND) 3 mice. Left panels: representative low magnification brightfield images of oviductal, uterine, and cervical organoids (scale bars, 100 μ m; inset 20 μ m). Right panels: immunofluorescent localization of CDH1 in female reproductive tract tissues (scale bars 100 μ m), insets represent single-layered epithelium in the oviduct and uterus and stratified epithelium in the cervix (scale bars, 10 μ m). Epi, epithelium; Mes, mesenchyme. (B) Representative low magnification brightfield images of endometrial epithelial organoids (EEO) established from PNDs 3, 5, 7, 12, and 15 (scale bars, 100 μ m). (C) Representative low magnification brightfield images of PND3 EEO cultured in WNT-containing media or WNT-deficient media (scale bars, 500 μ m), insets represent single-layered or multilayered EEOs in both culture conditions (scale bars, 100 μ m). A total of 25000 cells per drop were initially seeded across all groups. All brightfield images are representative of passage 3 organoids ($n \geq 3$ biological replicates per PND).

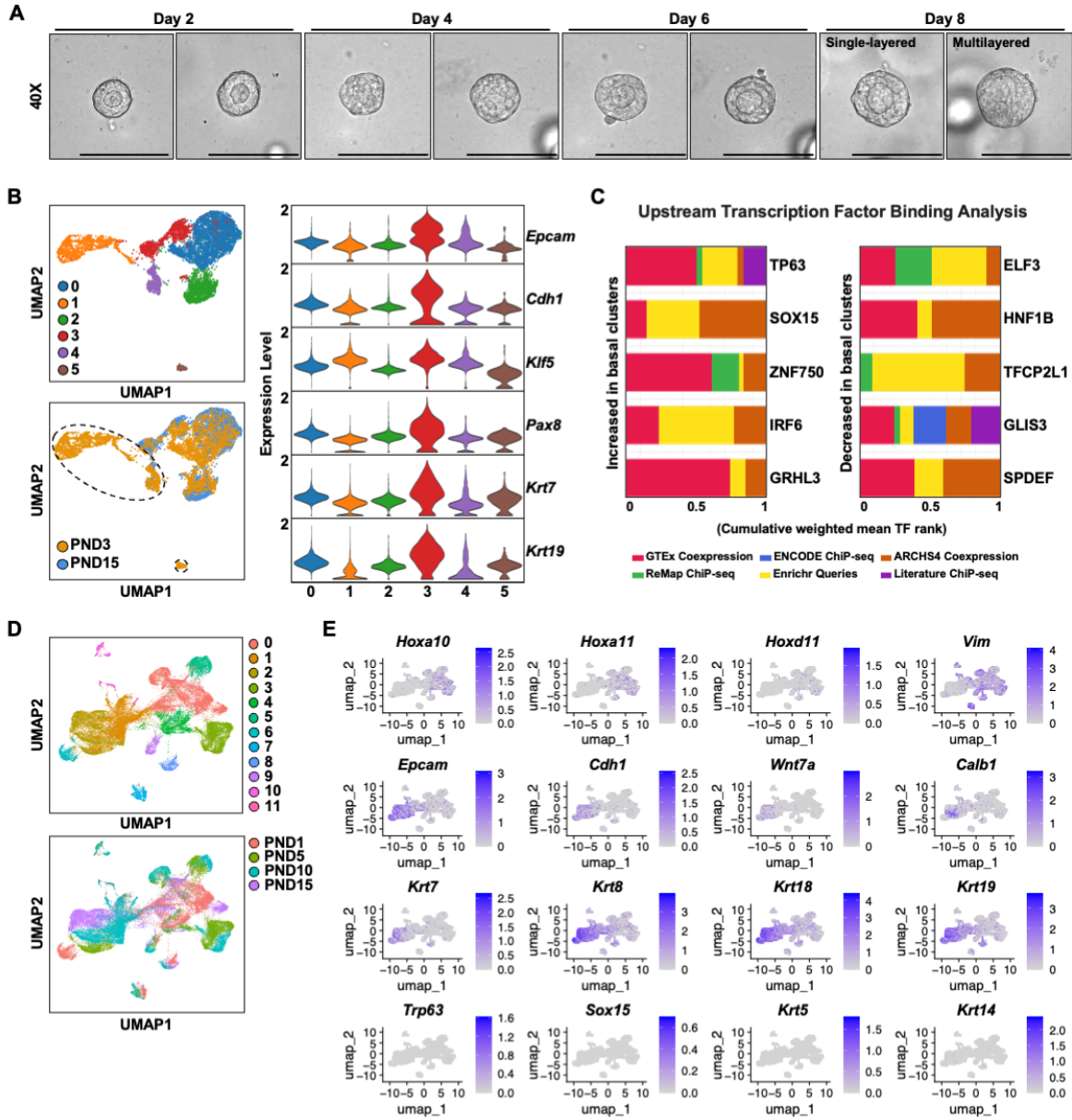


Figure S2. Cellular heterogeneity of neonatal endometrial epithelial organoids.

(A) Representative images of PND 3 EEO development over 8 days (scale bars, 100 μ m). (B) EEO established from PNDs 3 and 15 ($n = 10$ mice per PND) were collected after 8 days of culture and used for single cell RNA sequencing. Uniform Manifold Approximation and Projection (UMAP) plots show cells colored by cell type (top left) or PND (bottom left); circled clusters represent basal and ciliated epithelium present only in the PND3 samples. Violin plots represent the annotation of epithelial cell types based on known marker genes (right). (C) Top predicted upstream transcription factors underlying gene expression differences in the basal EEO clusters. (D) UMAP plots of uterine tissues from PNDs 1, 5, 10, and 15(15) show cells colored by cell type (top) or PND (bottom). (E) UMAPs of transcripts for the basal cell markers *Trp63*, *Sox15*, *Krt5*, and *Krt14* confirm the absence of basal epithelial cells in the neonatal uterine epithelium.

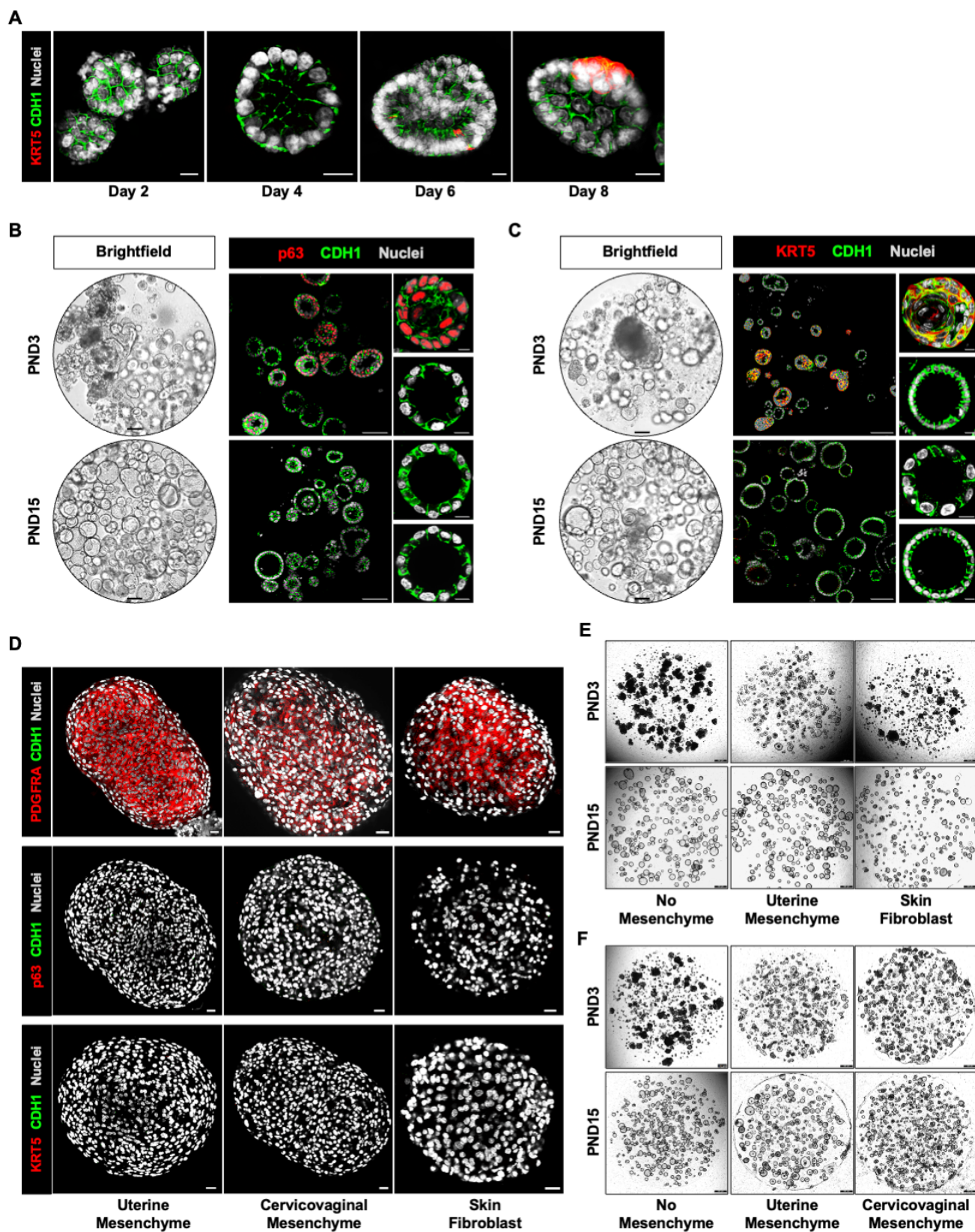


Figure S3. Mesenchymal induction of uterine luminal epithelial fate.

Whole mount immunofluorescent localization for the basal cell marker KRT5 in endometrial epithelial organoids (EEO) established from postnatal day (PND) 3 mice and cultured for 8 days (scale bars, 10 μ m). (B-C) Endometrial epithelium-only controls were established from PNDs 3 and 15 mice and cultured in 10% Cultrex for 8 days. Left panels: representative low magnification brightfield images (scale bars, 100 μ m). Right panels: immunofluorescent localization of (B) p63 and (C) KRT5 (scale bars 100 μ m). Insets show expression of basal cell markers restricted to the PND3 epithelium-only controls (scale bars, 10 μ m). The proportion of single- and multi-layered structures was calculated based on p63/KRT5 staining $[(\# \text{ of p63}^+/\text{KRT5}^+ \text{ EEO}) \div (\# \text{ of CDH1}^+ \text{ EEO})]$. Statistical differences between two groups were determined with Student's t-test ($p < 0.05$). (D) Mesenchyme/fibroblast-only aggregates were generated from PND3 uterus, cervix/vagina, and skin. Immunofluorescent localization of PDGFRA, CDH1, p63, and KRT5 confirms the absence of epithelial cells in mesenchyme-only aggregates (scale bars, 10 μ m). (E-F) For 2D coculture experiments, epithelial cells were seeded in Cultrex on transwell inserts over a bed of PND3 mesenchyme/fibroblasts adhered to the bottom of 6 well plates. Brightfield images show representative EEO cocultured with uterine mesenchyme and (E) skin fibroblast or (F) cervicovaginal mesenchyme at day 20 of culture (scale bars, 500 μ m).

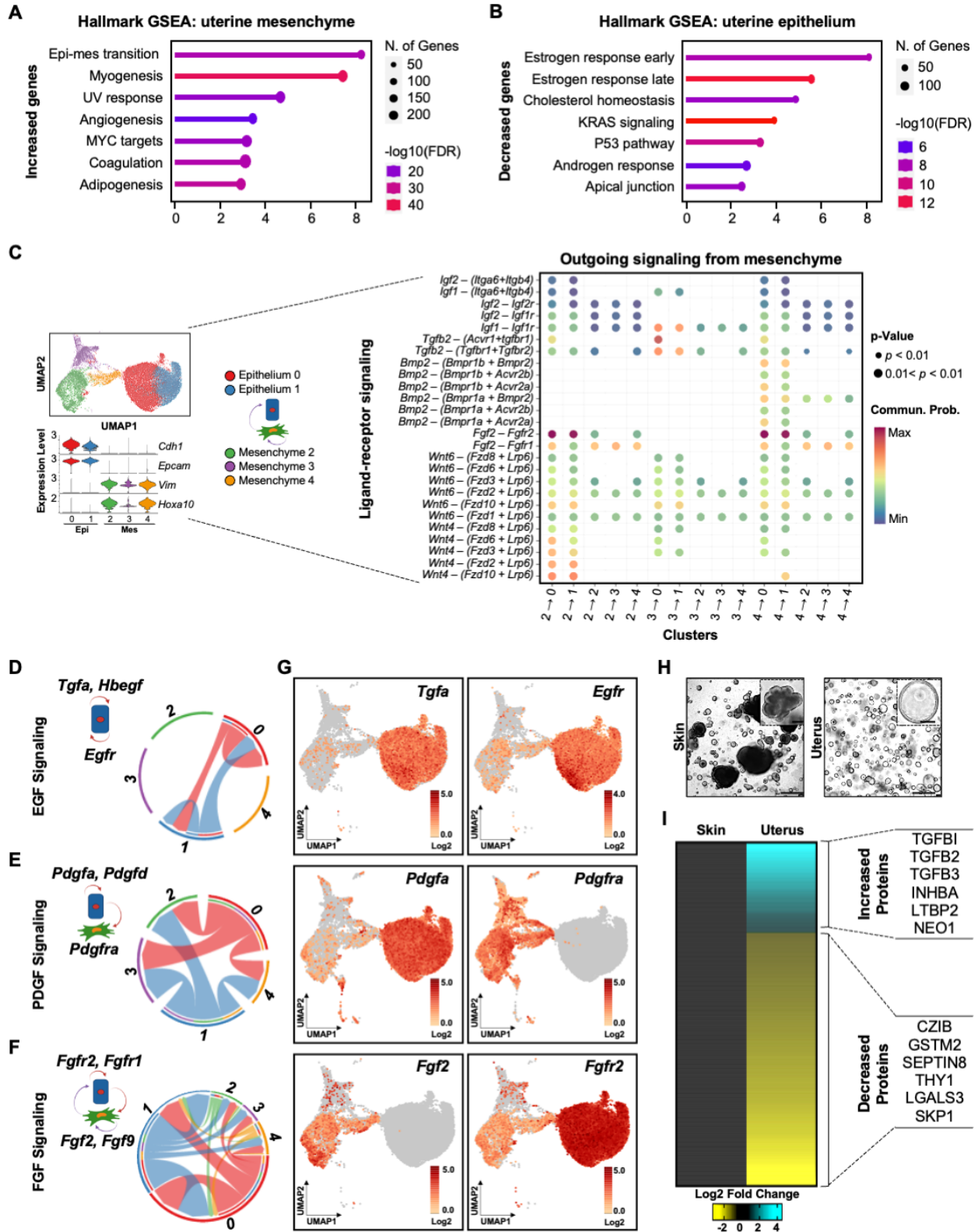


Figure S4. Epithelial and mesenchymal crosstalk governs neonatal uterine development.

(A) Visualization of hallmark gene set enrichment analysis (GSEA) associated with increased genes for uterine mesenchyme (left) and epithelium (right). (B) UMAP plot of integrated scRNA-seq analysis of mesenchyme (9) and epithelium (6) from neonatal uteri (top left). Violin plots represent annotation of cell types based on known marker genes (bottom left). Ligand-receptor pairs associated with outgoing signals from mesenchymal to epithelial cells. Shading denotes the relative communication probability across cell types. (D-F) Schematic of autocrine or paracrine signaling between epithelial and mesenchymal cells for selected pathways. (G) UMAP plots confirm the expression of ligands and receptors in each cell type. (H) Representative brightfield images illustrating the impact of skin fibroblast and uterine mesenchyme on endometrial epithelial organoid development (scale bars, 500 μ m); insets show single-layered and multilayered organoids (scale bars, 100 μ m). (I) Heatmap of differentially abundant TGFB pathway proteins determined by mass spectrometry analysis of uterine mesenchyme and skin fibroblast conditioned media.

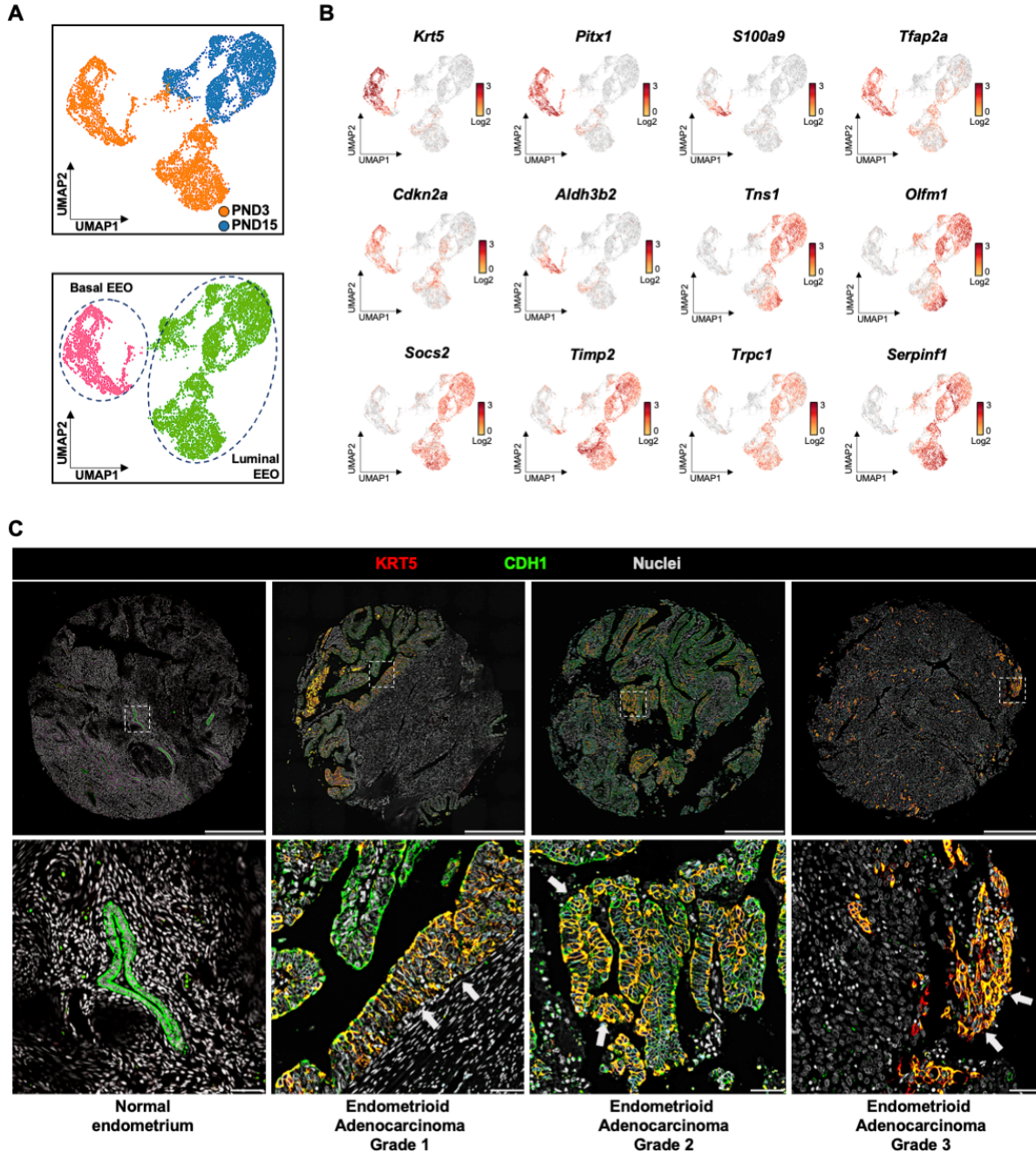


Figure S5. Conserved epithelial dynamics between uterine development and disease. (A) UMAP plots of endometrial epithelial organoids (EEO) subset into luminal and basal cell type clusters show cells colored by postnatal day (PND; top) and cluster type (bottom). (B) UMAPs of transcripts for genes with similar expression patterns between EEO and human Uterine Corpus Endometrial Carcinoma obtained from The Cancer Genome Atlas program database. (C) Immunofluorescent localization of KRT5 in tissues of patients with different grades of endometrioid adenocarcinoma (top panels, scale bars, 500 μ m), white arrows in the insets (bottom panels) indicate the presence of KRT5-positive epithelial cells (scale bars, 50 μ m).

Table S1. Base organoid media

Reagent	Source	Final concentration	Amount
Advanced DMEM/F12	Gibco; Cat#12634010	1X	479 mL
B27 Supplement	Gibco; Cat#12587010	1X	10 mL
Insulin-transferrin-selenium	Gibco; Cat#41400045	1X	5 mL
Primocin	InvivoGen; Cat# Ant-pm	100 µg/mL	1 mL
Glutamax	Gibco; Cat#35050061	1X	5 mL
Total		1X	500 mL

Note: Can be prepared in advance and stored up to 1 month at 4°C.

Table S2. Mouse organoid expansion media

Reagent	Source	Final concentration	Amount
Base organoid media		1X	196.4 mL
A83-01	Gibco; Cat#21041025	500 nM	200 µL
Murine EGF	BioGems; Cat#9094360	50 ng/mL	200 µL
Murine FGF-10	Preprotech; Cat#AF31509	100 ng/mL	200 µL
Murine R-spondin1	Preprotech; Cat#450-61	200 ng/mL	200 µL
Murine Noggin	Preprotech; Cat#315-32	100 ng/mL	200 µL
Murine Wnt3a	Preprotech; Cat# AF-250-38	50 ng/mL	200 µL
Nicotinamide	Preprotech; Cat# AF-315-20	1 mM	400 µL
N2	BioGems; Cat#9899208	1X	2 mL
Total			200 mL

Note: Can be prepared in advance and stored up to 2 weeks at 4°C.

Table S3. Stroma cell growth media.

Reagent	Source	Final concentration	Amount
Advanced DMEM/F12	Gibco; Cat#12634010	1X	440 mL
Fetal Bovine Serum (FBS)	Sigma; Cat#F2442	10%	50 mL
Glutamax	Gibco; Cat#35050061	1X	5 mL
Antibiotic-Antimycotic	Gibco; Cat#15240062	1%	5 mL
Total			500 mL

Note: Can be prepared in advance and stored up to 1 month at 4°C.

Table S4. Antibodies used in the study

Target	Dilution	Use	Supplier	Catalog No.	RRID
Mouse monoclonal anti-CDH1	1:500	IF	BD Biosciences	610182	RRID: AB_397581
Rabbit polyclonal anti-KI67	1:500	IF	Abcam	ab15580	RRID: AB_443209
Rabbit monoclonal anti-p63	1:500	IF	Cell Signaling	39692	RRID: AB_2799159
Rabbit monoclonal anti-KRT5	1:500	IF	Abcam	ab52635	RRID: AB_869890
Rabbit polyclonal anti-KRT14	1:500	IF	LS Bio	ls-B3916	RRID: AB_10662336
Mouse monoclonal anti-KRT8	1:200	IF	DSHB	ab531826	RRID: AB_531826
Rabbit monoclonal anti-Vimentin	1:500	IF	Cell Signaling	5741	RRID: AB_10695459
Rabbit monoclonal anti-PDGFR α	1:500	IF	Cell Signaling	3174	RRID: AB_2162345
Alexa Fluor 488, anti-rat IgG	1:500	IF	Jackson ImmunoResearch	112545143	RRID: AB_2338361
Alexa Fluor 647, anti-rabbit IgG	1:500	IF	Jackson ImmunoResearch	111605144	RRID: AB_2338078

Dataset S1. Differential gene expression between clusters of EEO (separate file).

Dataset S2. Differential protein secretion between skin fibroblast and uterine mesenchymal cells from postnatal day 3 female mice (separate file).

Dataset S3. MS2 protein abundance (separate file).

Dataset S4. Differential gene expression of endometrial cancer stroma and epithelium from Ren et al. (19) (separate file).

SI REFERENCES

1. J. A. Rizo, K. M. Davenport, W. Winuthayanon, T. E. Spencer, A. M. Kelleher, Estrogen receptor alpha regulates uterine epithelial lineage specification and homeostasis. *iScience* **26**, 107568 (2023).
2. J. A. Rizo, T. E. Spencer, A. M. Kelleher, Protocol for the establishment and characterization of an endometrial-derived epithelial organoid and stromal cell co-culture system. *STAR Protoc* **5**, 102894 (2024).
3. M. Y. Turco *et al.*, Long-term, hormone-responsive organoid cultures of human endometrium in a chemically defined medium. *Nat Cell Biol* **19**, 568-577 (2017).
4. H. C. Fitzgerald, P. Dhakal, S. K. Behura, D. J. Schust, T. E. Spencer, Self-renewing endometrial epithelial organoids of the human uterus. *Proc Natl Acad Sci U S A* **116**, 23132-23142 (2019).
5. J. F. Dekkers *et al.*, High-resolution 3D imaging of fixed and cleared organoids. *Nat Protoc* **14**, 1756-1771 (2019).
6. T. E. Spencer, M. T. Lowke, K. M. Davenport, P. Dhakal, A. M. Kelleher, Single-cell insights into epithelial morphogenesis in the neonatal mouse uterus. *Proc Natl Acad Sci U S A* **120**, e2316410120 (2023).
7. G. C. Linderman *et al.*, Zero-preserving imputation of single-cell RNA-seq data. *Nat Commun* **13**, 192 (2022).
8. R. Satija, J. A. Farrell, D. Gennert, A. F. Schier, A. Regev, Spatial reconstruction of single-cell gene expression data. *Nat Biotechnol* **33**, 495-502 (2015).
9. S. Jia, F. Zhao, Single-cell transcriptomic profiling of the neonatal oviduct and uterus reveals new insights into upper Müllerian duct regionalization. *FASEB J* **38**, e23632 (2024).
10. I. Korsunsky *et al.*, Fast, sensitive and accurate integration of single-cell data with Harmony. *Nat Methods* **16**, 1289-1296 (2019).
11. A. B. Keenan *et al.*, ChEA3: transcription factor enrichment analysis by orthogonal omics integration. *Nucleic Acids Res* **47**, W212-W224 (2019).
12. S. X. Ge, D. Jung, R. Yao, ShinyGO: a graphical gene-set enrichment tool for animals and plants. *Bioinformatics* **36**, 2628-2629 (2020).
13. A. Subramanian *et al.*, Gene set enrichment analysis: a knowledge-based approach for interpreting genome-wide expression profiles. *Proc Natl Acad Sci U S A* **102**, 15545-15550 (2005).
14. V. K. Mootha *et al.*, PGC-1alpha-responsive genes involved in oxidative phosphorylation are coordinately downregulated in human diabetes. *Nat Genet* **34**, 267-273 (2003).
15. H. Bao *et al.*, PR-SET7 epigenetically restrains uterine interferon response and cell death governing proper postnatal stromal development. *Nat Commun* **15**, 4920 (2024).
16. S. Jin *et al.*, Inference and analysis of cell-cell communication using CellChat. *Nat Commun* **12**, 1088 (2021).
17. N. Kumar *et al.*, Decoding spatiotemporal transcriptional dynamics and epithelial fibroblast crosstalk during gastroesophageal junction development through single cell analysis. *Nat Commun* **15**, 3064 (2024).
18. C. Hutter, J. C. Zenklusen, The Cancer Genome Atlas: Creating Lasting Value beyond Its Data. *Cell* **173**, 283-285 (2018).
19. X. Ren *et al.*, Single-cell transcriptomic analysis highlights origin and pathological process of human endometrioid endometrial carcinoma. *Nat Commun* **13**, 6300 (2022).